PROCEEDINGS, 41st Workshop on Geothermal Reservoir Engineering
Stanford University, Stanford, California, February 22-24, 2016
SGP-TR-209

Rock Physics Modeling for the Potential FORGE Site on the Eastern Snake River Plain, Idaho

Dario Grana[1+], Sumit Verma[1], Robert Podgorney[2]

[1] Department of Geology and Geophysics, University of Wyoming, Laramie, WY 82070

[2] Idaho National Laboratory, Idaho Falls, ID 83415

[+] Corresponding author: dgrana@uwyo.edu

Keywords: Rock physics, Seismic modeling, Snake River Plane

ABSTRACT

Rock physics models allow establishing a physical-mathematical relation between rock and fluid properties and geophysical attributes. In this study, we propose to apply rock physics models to a geophysical dataset measured at two well locations near the proposed Snake River Plain FORGE site in eastern Idaho. The potential target is a rhyolite layer, which occurs between 2,000 and 3,000 m. The available data include two sets of sonic and petrophysical well logs at two well locations, which are approximately 6 km apart. The goal of this study is to calibrate a physical model to link reservoir properties (porosity, lithology, saturation) and reservoir conditions (pressure and temperature) with geophysical attributes (velocities, density, and resistivity). This multi-physics model is calibrated at the well locations, but can be extended to the entire site if geophysical data are available. As a feasibility study to determine the value of information of 3D geophysical surveys we plan to build synthetic 2D sections through the two existing wells by interpolating well log data using geostatistical techniques such as kriging and sequential Gaussian simulations and compute the predicted seismic, electromagnetic and gravimetric responses of the model. By combining rock physics models with mathematical inverse theory, we plan to perform a sensitivity analysis on the resolution and noise level of the geophysical survey in order to determine the minimum requirements of the geophysical data acquisition to improve the reservoir description. We will also compare the new results with a previous study based on 2D refraction seismic, resistivity and gravity fields.

1. INTRODUCTION

Rock physics modeling is the discipline that studies physical-mathematical relations between geophysical measurements, such as elastic properties of seismic waves, and rock and fluid properties, such as porosity, lithology and fluid saturations. Geophysical measurements do not contain direct measurements of the reservoir properties. Indeed seismic data contain information about the compressional and shear wave velocity; electromagnetic surveys include resistivity measurements; and gravity surveys provide density data. Therefore, in hydrocarbon reservoir modeling, these sets of relations are essential to estimate rock and fluid properties from geophysical attributes and build 3-dimentional models for fluid flow simulations and predictions. Similarly, in geothermal reservoirs, we can apply rock physics models to build an initial static model for geothermal dynamic simulations.

Rock physics literature includes several models to estimate elastic and electrical properties from rock and fluid measurements (Mavko et al., 2009; Dvorkin et al., 2014). For example, given a set of rock physics relations, we can estimate the velocity of compressional and shear waves given the porosity, lithological content and fluid saturation of the porous rock at reservoir conditions. Similarly, we can also estimate the resistivity and density of the porous rock. Rock physics provides several empirical and physically-derived relations to estimate the link between porosity and velocity, porosity and permeability, saturation and resistivity for a number of lithologies and fluid mixtures. Datasets acquired in hydrocarbon reservoirs show common trends between these properties. Once a relation between geophysical attributes and rock and fluid properties is established, we can then quantitatively interpret geophysical measurements and build 3-dimentional models. Rock physics models can be also used for feasibility studies for acquisition of geophysical datasets. The rock physics model can reveal which geophysical survey is the most sensitive to rock and fluid properties, and determine which geophysical dataset should be acquired in the field.

In general, a rock physics model includes multiple relations. When we create a poroelastic model for porous rocks, we first model the solid and fluid phase independently and then we model the poroelastic properties of the saturated rock as a mixture of the solid and fluid phases. Each phase is modeled as an effective medium. Mixing laws are available in literature, such as Voigt and Reuss averages and Hashin Shtrikmann bounds (Mavko et al., 2009; Dvorkin et al., 2014). To combine the two phases, the model for the porosity effect depends on the rock type under study. Empirical relations such as Han's multilinear regression and Wyllie and Raymer's regressions can be applied (Mavko et al., 2009; Dvorkin et al., 2014). However, these relations must be fitted to real data in order to be extended to the entire dataset. Among the physical relations used to describe the porosity effect, two main categories of models can be distinguished: granular media models and inclusion models (Mavko et al., 2009; Dvorkin et al., 2014). In granular media models, we assume that the porous rock is a random pack of spherical grains and we try to mathematically approximate the compressibility of the rock. In inclusion models, we approximate the geometrical shape of the pores using spheres or ellipsoids and we estimate the rock compressibility. The fluid effect is generally included in the model through Gassmann's equations (Mavko et al., 2009; Dvorkin et al., 2014).

In this study, we aim to build a rock physics model for a geothermal reservoir and compute the potential seismic response for different reservoir scenarios. In this work, we focus on elastic properties and seismic data because of the higher resolution of seismic compared to electromagnetic and gravity data and the potential ability of seismic modeling and inversion to monitor the dynamic changes in the reservoir through time. However, the workflow can be extended to other geophysical measurements such as electromagnetic and gravity surveys if a suitable rock physics model can be calibrated at the well location. Seismic attributes can be measured at the well location and can be derived from 3-dimentional seismic data through seismic inverse modeling methods (Aki and Richards, 1980 and Yilmaz, 2001).

The dataset under study is the Potential FORGE Site on the Eastern Snake River Plain, Idaho. The Snake River is located along the track of the Yellowstone Hot Spot. The site is characterized by high heat flow and subsurface temperatures, a prolific regional aquifer system, and favorable regional stress and seismic conditions (Podgorney et al., 2016; Plummer et al., 2016; and Neupane et al., 2016). The study was identified by a recent MIT study as one of the top locations for Enhanced Geothermal Systems in the United States (Podgorney et al., 2016). In this work, we show the preliminary geophysical study including the rock physics model calibration and seismic feasibility study. For the model calibration, w used the data measured at the INEL 1 well, 6 km away from the site.

2. METHOD AND APPLICATION

In this section, we present the rock physics analysis at the INEL 1 location and use the so-obtained results as a feasibility study for seismic acquisition and modeling. The goal of this work is to establish a set of physical-mathematical relations between geophysical measurements and rock and fluid properties. These relations can be then used to build 3-dimentional reservoir models once geophysical data are acquired. Indeed, these models allow the identification of lithologies and the estimation of porosity and potentially fluid saturations from seismic, electromagnetic and gravity data.

2.1 Dataset

The available set of well logs at the INEL 1 location includes gamma ray, density, sonic, neutron porosity and resistivity (Figure 1). A facies classification has been derived according to the stratigraphic profile presented in Doherty et al. 1979 (for further details also refer to McCurry and Rodgers, 2009, and Drew et al., 2013). A preliminary data processing and well log analysis has been performed on the data to eliminate biased measurements and reconstruct sections of the logs in which data were missing. In particular, a local multilinear regression has been used to reconstruct part of the density log. In the interval of interest, between 2000 and 3000 m, all the logs were measured correctly, and the caliper log does not show relevant anomalies in the borehole. Doherty et al. (1979) determined seven sedimentological facies, based on well cuttings and cores. According to regional geological models and stratigraphy, we simplified the model to five main lithological facies (Figure 1): a shallow section basalt interlayered with sand and silt layers; a deeper basalt layer consisting of welded tuff interlayered with thin layers of tuffaceous sand and air fall ash; and a dense, recrystallized, hydrothermally altered rhyodacite.

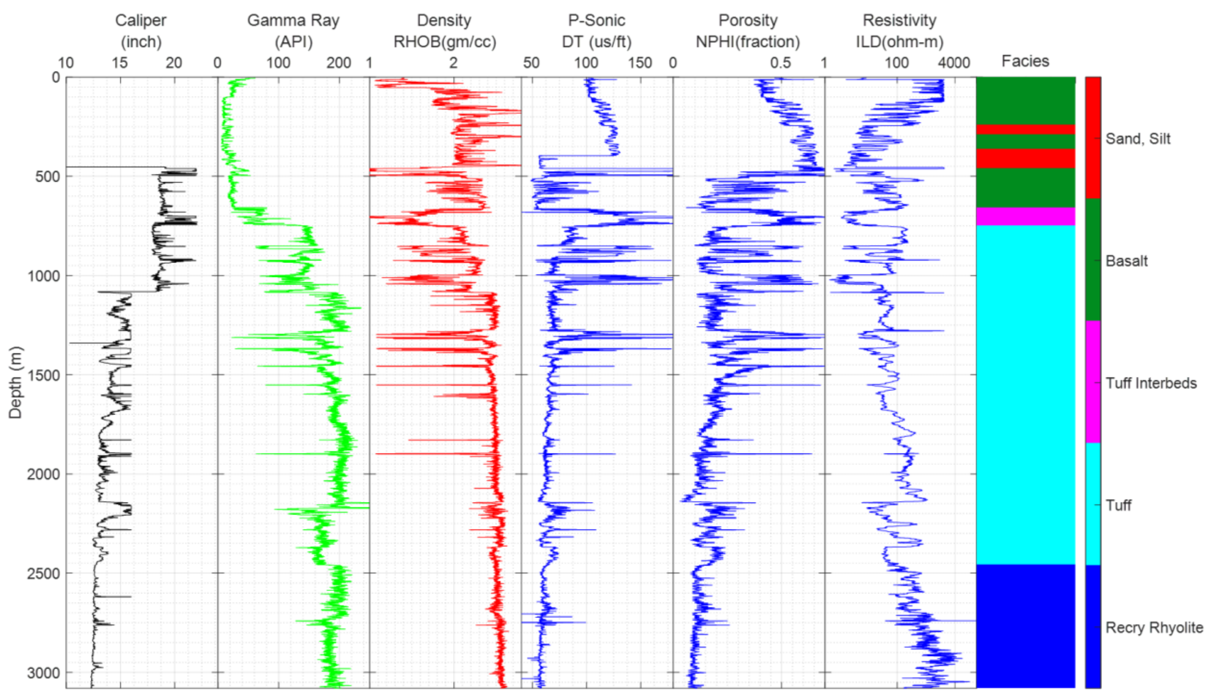

Figure 1: Well logs dataset at well INEL 1; from left to right: caliper, gamma ray, bulk density, sonic log, neutron porosity, deep induction log resistivity. A facies profile is shown in the last plot (the classification was derived and modified after Doherty et al., 1979).

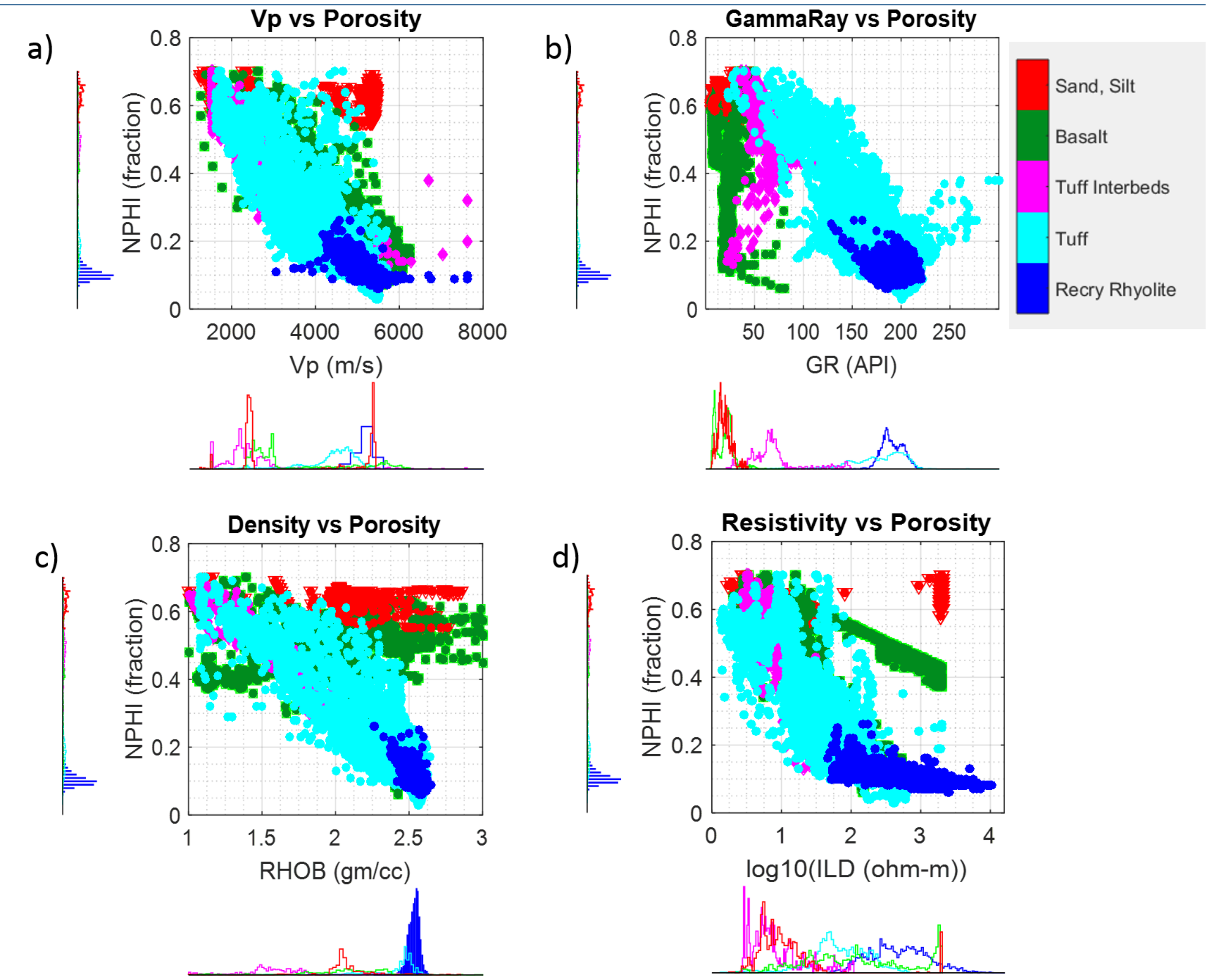

Figure 2: Crossplots between elastic and petrophysical properties versus porosity: (a) P-wave velocity, (b) Gamma ray, (c) Density and (d) Resistivity versus neutron porosity.

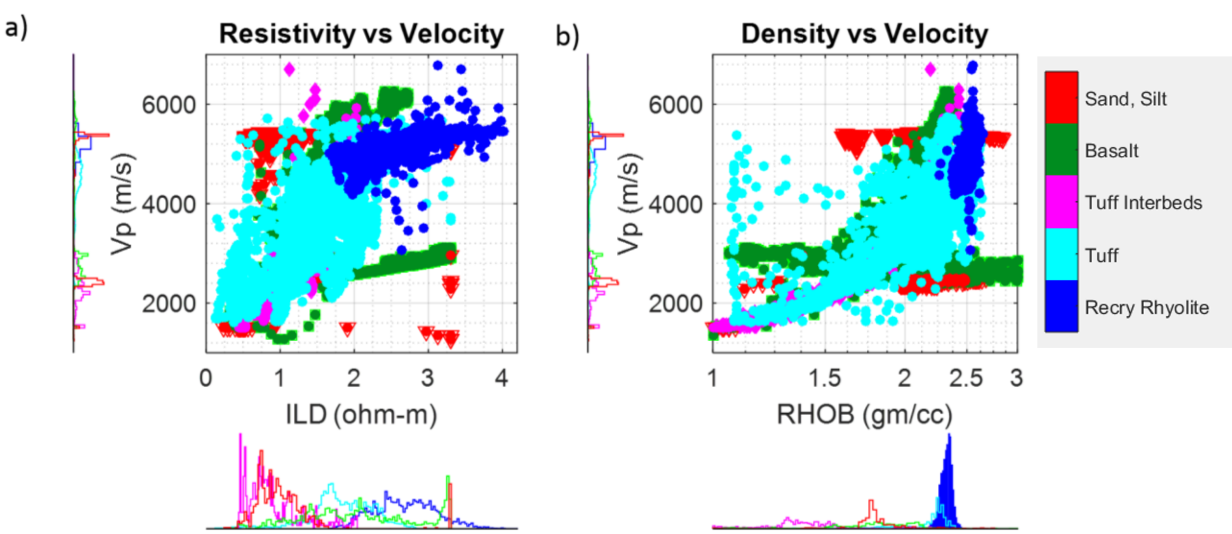

Figure 3: Crossplots in the joint elastic and electrical domains: (a) P-wave velocity versus resistivity and (b) P-wave velocity versus density.

According to the sonic log (Figure 1), the elastic responses of tuff and rhyolite show similar features. However, in a multivariate analysis the rhyolite layer can be discriminated from the tuff layer. In Figures 2 and 3, we show rock physics crossplots of well logs. In Figure 2 (top left), we show the relation between porosity and P-wave velocity. Although the well log data are noisy, the absolute value of the linear correlation between porosity and velocity is generally high. Porosity and velocity are anti-correlated in each facies. The relation is approximately linear in tuff and rhyolite; however, due to the lower porosity, rhyolite is distinguishable in this petro-elastic domain. The resolution of seismic data is lower than the resolution of well logs; however, if the linear relation between porosity and velocity is still valid at the seismic scale, we can estimate the porosity in the rhyolite layer from seismic attributes. A linear relation is observable also in the petrophysical domain porosity versus gamma ray (Figure 2, top right). The linear correlation is negative. Overall, the higher is the gamma ray, the lower is the neutron porosity. Rhyolite is characterized by high gamma ray and low porosity. Tuffaceous sand interbeds have a lower range of gamma ray compared to tuff. Because gamma ray and density are highly correlated, we expect the neutron porosity and density to be negatively correlated as well. Indeed the higher is the neutron porosity, the lower is the density (Figure 2, bottom left). In Figure 2 (bottom right), we show the relation between porosity and resistivity. Although there are several values in the plot that do not follow any trend and could be considered outliers due inaccurate measurements or mud effect, we see an exponential relation between porosity and resistivity. In particular, even if the porosity is low in the rhyolite, the resistivity is relatively high. This crossplot suggests that we could obtain a good lithological discrimination in the joint elastic-electric domain by combining the results of seismic inversion (i.e. elastic attributes such as velocity and density) and results of the electromagnetic inversion (i.e. resistivity). An additional constrain can be added if gravity data are available, to better determine the density model. In Figure 3, we analyze the joint elastic and electrical domain. The crossplot between P-wave velocity and resistivity shows a good discrimination between tuff and rhyolite; however, we point out that the resolution of the resistivity model that can be achieved from electromagnetic data is lower than the seismic resolution. The lower resolution could then affect the discriminability of the different facies. If the seismic acquisition includes large acquisition angles (or if gravity data are available), density could be estimated from seismic data. In Figure 3, we show that rhyolite can be discriminated in the acoustic-elastic domain as well.

In order to calibrate and apply a rock physics model to well log data, we preliminary filtered the well log data to eliminate noise and outliers. The filtered data are shown in Figure 4. A facies classification has been performed on filtered data based on a statistical algorithm, namely the expectation and maximization algorithm (Hastie et al., 2009). The statistical classification is consistent with the stratigraphic profile shown in Figure 1. However, rhyolite is over-predicted within the tuff layer; whereas the interbedded sand and silt layers are not identified. This classification can be potentially extended to the entire reservoir model if geophysical measurements are available. The resolution of the filtered logs is still higher than the seismic resolution; therefore, some of the thin layers might not be resolved by geophysical data.

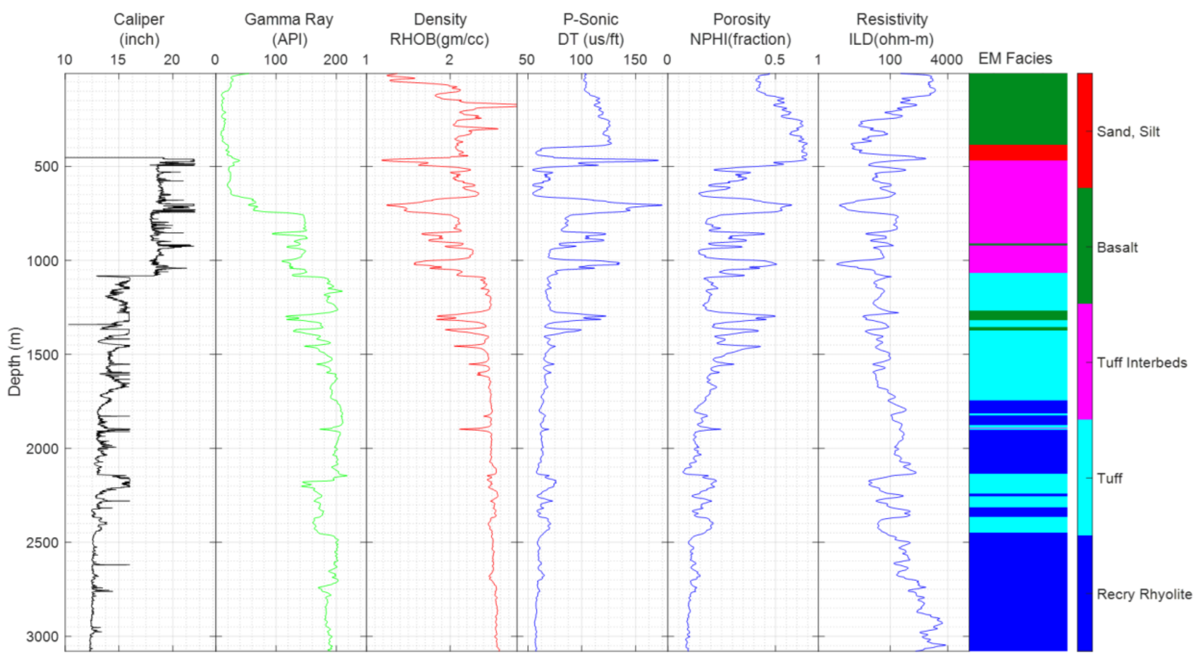

Figure 4: Filtered well logs from well INEL 1; from left to right: caliper, gamma ray, bulk density, sonic log, neutron porosity, deep induction log resistivity. A facies profile obtained using the expectation-maximization algorithm is shown in the last plot.

2.2 Rock physics model

In this section, we estimate a set of relations to link elastic and petrophysical parameters. Because rhyolite samples are not very common in hydrocarbon reservoir models, a limited number of measurements and physical-mathematical models are available in literature. In this study, we tested three different models: Nur's critical porosity, Raymers's equation, and the stiff sand model heuristically extended to rhyolite. For a complete description of these models, we refer the reader to Mavko et al. (2009). We applied these models to estimate the elastic moduli (bulk and shear moduli) of the dry rock in the tuff and rhyolite intervals. These models require the knowledge of the elastic properties of the solid rock. Due to the lack of elastic measurements on core samples, we tested several values and chose the optimal parameters based on the best fit between rock physics model predictions and measured data.

For this study, we selected the Nur's critical porosity model, although the other models provided consistent results. The fluid is assumed to be water in the entire interval of interest. The effect of the fluid on elastic properties can be described at the seismic scale by Gassmann's equation (Mavko et al., 2009). This model allows us to compute the bulk modulus of the saturated rock given its porosity, the bulk modulus of the solid phase, the bulk modulus of the dry rock, and the bulk modulus of the fluid. The shear modulus of the saturated rock is assumed to be the same as the shear modulus of the dry rock.

Nur's critical porosity model approximates the behavior of the dry rock with linear relations respect to porosity ϕ to compute the dry-rock elastic moduli K_{dry} and G_{dry}:

$$
\begin{aligned}
K_{dry} &= K_{mat}\left(1-\frac{\phi}{\phi_c}\right)\\
G_{dry} &= G_{mat}\left(1-\frac{\phi}{\phi_c}\right),
\end{aligned}
\qquad (1)
$$

where ϕ_c is the critical porosity of the rock (assumed to be equal to 0.6 in our study) and K_{mat} and G_{mat} are the elastic moduli of the solid phase.

The fluid effect is introduced by combining dry rock properties in Equation 1 with the fluid properties, to obtain the saturated rock elastic moduli K_{sat} and G_{sat} through Gassmann's equations:

$$
\begin{aligned}
K_{sat} &= K_{dry}+\frac{\left(1-\dfrac{K_{dry}}{K_{mat}}\right)^2}{\dfrac{\phi}{K_{fl}}+\dfrac{(1-\phi)}{K_{mat}}-\dfrac{K_{dry}}{K_{mat}^2}}\\
G_{sat} &= G_{dry},
\end{aligned}
\qquad (2)
$$

where K_{fl} is the bulk modulus of the fluid, which in our application is assumed to be water with bulk modulus of 2.25 GPa.

We applied the model in Equations 1 and 2 to the set of filtered well logs (Figure 4) to predict the elastic response of the reservoir. The predicted model is shown in Figure 5. One of the limitations of empirical rock physics models is the limited capability to predict S-wave velocity if well log data are not available for the calibration of the shear wave model. If S-wave velocity is required for the quantitative seismic interpretation study, a more reliable prediction could be obtained using the stiff sand model (Dvorkin et al., 2014).

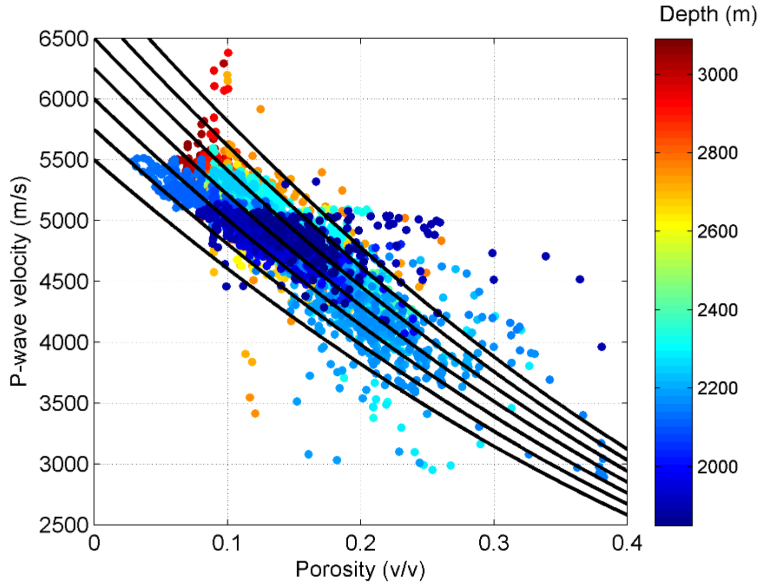

Figure 5: Rock physics model for predicting P-wave velocity as a function of porosity. Colored dots represent the well log measurements (color coded by depth), whereas the black curves show the rock physics model for several values of bulk modulus of the solid phase.

The stiff sand model (Dvorkin et al., 2014) is based on the modified Hashin–Shtrikman bound. The model combines the elastic moduli of the solid phase (rhyolite in our case) and Hertz-Mindlin moduli at the critical porosity ϕ_c. The Hertz-Mindlin equations allows us to compute the elastic moduli as follows:

$$
\begin{aligned}
K_{HM} &= \sqrt[3]{\frac{n^2(1-\phi_c)^2 G_{mat}^2}{18\pi^2(1-\nu)^2} P} \\
G_{HM} &= \frac{5-4\nu}{5(2-\nu)} \sqrt[3]{\frac{3n^2(1-\phi_c)^2 G_{mat}^2}{2\pi^2(1-\nu)^2} P},
\end{aligned}
\tag{3}
$$

where P is the effective pressure, n is the average number of contacts per grain and ν is the Poisson ratio.

For effective porosity values between zero and the critical porosity, the stiff sand model connects the elastic moduli of the solid phase to the Hertz-Mindlin moduli of the dry rock at porosity ϕ_c, by interpolating the two end members at the intermediate porosity values through the modified Hashin-Shtrikman upper bound:

$$
\begin{aligned}
K_{dry} &= \left(\frac{\frac{\phi}{\phi_c}}{K_{HM} + \frac{4}{3}G_{mat}} + \frac{1-\frac{\phi}{\phi_c}}{K_{mat} + \frac{4}{3}G_{mat}} \right)^{-1} - \frac{4}{3}G_{mat} \\
G_{dry} &= \left(\frac{\frac{\phi}{\phi_c}}{G_{HM} + \frac{1}{6}\xi G_{mat}} + \frac{1-\frac{\phi}{\phi_c}}{G_{mat} + \frac{1}{6}\xi G_{mat}} \right)^{-1} - \frac{1}{6}\xi G_{mat}, \qquad \xi = \frac{9K_{mat} + 8G_{mat}}{K_{mat} + 2G_{mat}}
\end{aligned}
\tag{4}
$$

We point out that the above-mentioned rock physics models do not include a geometrical description of the pore shape and treat the pore space as an effective medium. Furthermore, the measured data do not provide any information about the potential fracture system. A more accurate prediction could be obtained by integrating geomechanical measurements such as crack density and orientation in the rock physics model. Geomechanical analysis of the reservoir rocks are presented in Bakshi and Ghassemi (2016).

2.3 Seismic model and feasibility study

In this section, we apply a linearized seismic forward model to compute the seismic response of the reservoir layer and the sealing layer above it. If the elastic properties of the upper and lower layers are known, then the seismic response can be computed as a convolution of a wavelet and the reflection coefficients of the layer interface. The exact expression of the reflection coefficients can be computed using Zoeppritz equations (Aki and Richards, 1980); however, in this application, we assume that the incident angle is smaller than 45 degrees and the contrast of the elastic properties between the upper and lower layer is small, in order to apply a linearized approximation of Zoeppritz equations for weak contrasts. We use a three term approximation, namely Aki-Richards equation (Aki and Richards, 1980). In this synthetic example, we assume a Ricker wavelet with dominant frequency of 30 Hz. The predicted seismic response is shown in Figure 6 (left). A sensitivity study on the parameters affecting the quality of seismic data has been performed to verify the applicability of a seismic inversion approach to estimate the elastic properties in the reservoir and potentially the petrophysical parameters. The accuracy of the inversion results depend on the signal to noise ratio of the seismic dataset, the dominant frequency of the wavelet, the number of available angle stacks and the maximum angle. In particular, the estimation of density from seismic data requires a large incident angle in order to obtain accurate results.

The synthetic study has been performed using the petroelastic properties at reservoir conditions. The aim of the second part of the study is to verify the feasibility of reservoir monitoring through time-lapse seismic surveys. For this reason, we mimic a potential production scenario where reservoir water is replaced by steam. The elastic response has been computed using Gassmann's equations (Equation 2). In this example, we assume that porosity does not change during production. This assumption is conservative and aims to study the fluid effect only. If porosity increases due to hydraulic fracturing, the fluid effect on seismic variations will be more significant. The seismic response at the well location in the new reservoir scenario is shown in Figure 6 (mid plot). It is important to notice that we do not only observe a change in seismic amplitudes but also in the travel time. However, in order to compute the difference between the two seismic datasets, we must apply a time-shift correction using a warping technique (Figure 6, right plot). The difference in the two datasets can then be used for quantitative interpretation of time-lapse seismic data and reservoir monitoring. In this dataset, the velocity in rhyolite filled by steam decreases compared to the velocity in rhyolite filled by water due to the larger compressibility of steam compared to water.

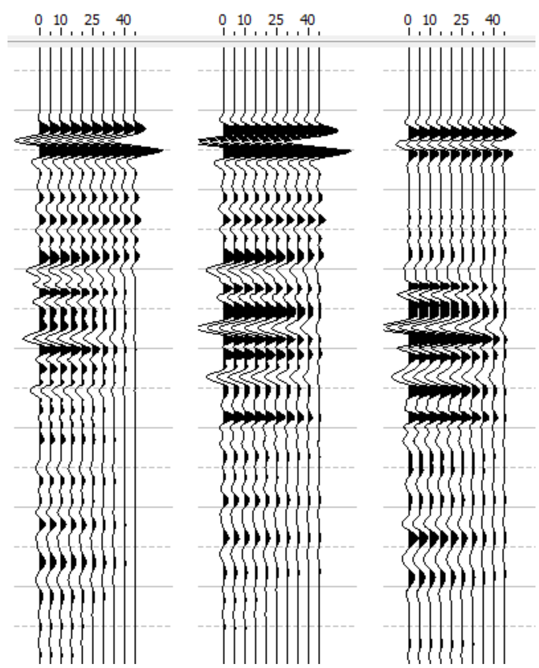

Figure 6: Synthetic seismic dataset between 2,000 and 3,000 meters. The left plot shows synthetic seismic at reservoir conditions; the mid plot shows synthetic seismic in steam conditions (same porosity as reservoir conditions). The seismic dataset in the mid plot has been corrected for time-shift to make it comparable to the left plot. Seismic differences (after time-shift correction) are shown in the right plot.

The feasibility study shows that seismic data can be used to constrain a 3D reservoir model of petrophysical properties, such as porosity, as well as to monitor saturation changes in the reservoir through time-lapse surveys. Electromagnetic and gravity surveys can be included in the reservoir characterization workflow; however, the resolution of these datasets is generally lower than the resolution of seismic data. For the characterization of the static reservoir model, seismic data should provide the most reliable information as long is the signal to noise ratio is large enough. A seismic dataset has been acquired in the 80s (see Sparlin et al., 1982 and Pankratz and Ackermann, 1982). An interpreted 2D section is shown in Figure 7 (left plot). However, this dataset only contains refraction seismic data. Therefore, the main interface between tuff and rhyolite cannot be interpreted from the data, due to the negative reflectivity at the interface. Gravity and resistivity data are also available. Sparlin et al. (1982) and Pankratz and Ackermann (1982) show an interpreted gravity section to estimate density (Figure 7, right plot). The integrated interpretation is based on a linear relation between velocity and density, which is confirmed by the well log data at INEL 1 location (Figure 3, right plot). For reservoir monitoring, both gravity and electromagnetic data could be used to estimate the spatial distribution of water and steam; however, a feasibility study prior to data acquisition is required to investigate the limitations due to data resolution.

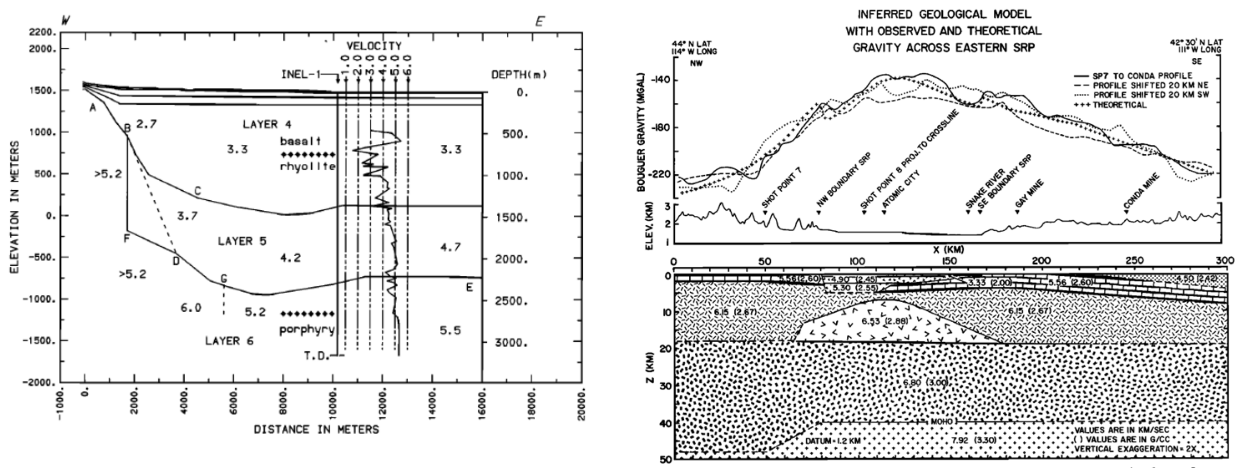

Figure 7: Interpretation of refraction seismic data (left plot) and gravity data (right plot) from Sparlin et al. (1982) and Pankratz and Ackermann (1982).

3. CONCLUSIONS

In this work, we presented a reservoir modeling workflow aimed to quantitatively interpret well log and surface geophysical measurements. The workflow includes a rock physics model to link the rock and fluid properties to elastic attributes such as seismic velocity and density; whereas, the seismic modeling includes a convolutional model and a linearized approximation of the reflection coefficient model to estimate the seismic signature of the reservoir rocks. This forward model is calibrated at the well location and can be integrated in an inversion workflow to estimate rock and fluid properties from geophysical measurements, such as surface seismic and eventually electromagnetic and gravity data. The study also aims to assess the ability of time-lapse seismic data to monitor dynamic changes in the reservoir fluids. In particular, time-lapse seismic differences can be used to estimate the spatial distribution of water and steam at different time steps of the production process.

REFERENCES

Aki, K., and Richards, P. G.: Quantitative seismology: *W. H. Freeman & Co* (1980).

Bakshi, R., and Ghassemi, A.: Geomechanical Characterization of Rock Core from the Proposed FORGE Laboratory on the Eastern Snake River Plain, Idaho: 41st workshop on Geothermal Reservoir Engineering, Stanford University, Stanford, CA (2016).

Doherty, D.J., McBroome, L.A., and Kuntz, M.: Preliminary geological interpretation and lithologic log of the exploratory geothermal test well (INEL-1), Idaho National Engineering Laboratory: *U.S. Geological Survey,* **9**, Open File Report, (1979), 79–1248.

Drew, D.L, Bindeman, I.N., Watts, K.E., Schmitt, A.K., Fu, B. and McCurry, M.: Crustal-scale recycling in caldera complexed and rift zones along the Yellowstone hot spot track: O and Hf isotopic evidence in diverse zircons from voluminous rhyolites of the Picabo volcanic field, Idaho: *Earth and Planetary Science Letters,* **381**, (2013), 63–77.

Dvorkin, J., Gutierrez, M., and Grana, D.: Seismic reflections of rock properties: *Cambridge University Press* (2014).

Hastie, T., Tibshirani, R., and Friedman, J.: The elements of statistical learning: *Springer* (2009).

Mavko, G., Mukerji, T., and Dvorkin, J.: The rock physics handbook: *Cambridge University Press* (2009).

McCurry, M., and Rodgers, D.W.: Mass transfer along the Yellowstone hotspot track I: Petrologic constraints on the volume of mantle-derived magma: *Journal of Volcanology and Geothermal Research*, **188**, (2009), 86–98

Neupane, G., Mattson, E.D., Cannon, C.J., Atkinson, T.A., Mcling, T.L., Wood, T.R., Dobson, P.F., and Conrad M.E.: Potential Hydrothermal Resource Temperatures in the Eastern Snake River Plain, Idaho: Plummer, M., Palmer, C.D., Mcling, T., and Sondrup A.J.: Modeling Heat Flow in the Eastern Snake River Plain Aquifer: 41st workshop on Geothermal Reservoir Engineering, Stanford University, Stanford, CA (2016).

Pankratz, L.W., and Ackermann, H.D.: Structure along the northwest edge of the Snake River Plain interpreted from seismic refraction: *Journal of Geophysical Research: Solid Earth*, **87**, (B4), (1982), 2676-2682.

Plummer, M., Palmer, C.D., Mcling, T., and Sondrup A.J.: Modeling Heat Flow in the Eastern Snake River Plain Aquifer: 41st workshop on Geothermal Reservoir Engineering, Stanford University, Stanford, CA (2016).

Podgorney R., Snyder, N., and Roy, M.: A Snake River Plain Field Laboratory for Enhanced Geothermal Systems: an Overview of the Snake River Geothermal Consortium's Proposed FORGE Approach and Site: 41st workshop on Geothermal Reservoir Engineering, Stanford University, Stanford, CA (2016).

Sparlin, M.A., Braile, L.W., and Smith, R.B.: Crustal structure of the eastern Snake River Plain determined from ray trace modeling of seismic refraction data: *Journal of Geophysical Research: Solid Earth*, **87**, (B4), (1982), 2619-2633.

Yilmaz, Ö.: Seismic data analysis: *Society of exploration geophysicists* (2001).

.